ZIBELINE INTERNATIONAL™ PUBLISHING

ISSN: 2521-0920 (Print)
ISSN: 2521-0602 (Online)
CODEN: MJGAAN

Malaysian Journal of Geosciences (MJG)

DOI: http://doi.org/10.26480/mjg.01.2024.59.75

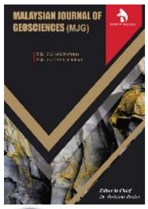

RESEARCH ARTICLE

UTILISING 2-D RESISTIVITY IMAGING TOMOGRAPHY IN INVESTIGATING STRUCTURAL FAILURE IN SOME BUILDINGS IN ADANKOLO CAMPUS OF FEDERAL UNIVERSITY LOKOJA, NIGERIAN NORTH CENTRAL AREA

Abdulbariu Ibrahim[a*], Jafaru Nasiru[a], Mu'awiya Baba Aminu[a,b*], Ayinla Habeeb Ayoola[a], Mojeed Olaniyi Fasasi[c], Yinka Benjamin Oluwadiya[d]

[a] *Department of Geology, Federal University Lokoja, Kogi State, Nigeria.*
[b] *School of Materials and Mineral Resources Engineering, Universiti Sains Malaysia, Malaysia.*
[c] *Scott Sutherland School of Architecture & Built Environment, Robert Gordon University, United Kingdom.*
[d] *Civil, Construction, and Environmental Engineering, School of Engineering, Marquette University, USA.*
**Corresponding Author Email: abdulbariu.ibrahim@fulokoja.edu.ng; muawiya.babaaminu@fulokoja.edu.ng*

ARTICLE DETAILS

Article History:

Received 20 February 2024
Revised 04 March 2024
Accepted 23 April 2024
Available online 25 April 2024

ABSTRACT

One of the most used geophysical tools for characterization of the near surface is electrical resistivity tomography (ERT). The 2D resistivity survey was conducted along ten (10) buildings in Federal University Lokoja (Fulokoja), Adonkolo Campus. Dipole-dipole electrode configuration was conducted for data collection. Enhancing of measured field and calculated apparent resistivity details/data and interpretation of Electrical Resistivity Tomography (ERT) were generated using RES2DINV software which reveal a change in soil resistivity and type. From the result it is observed that the soil is made up of weathered migmatite rock which exist in layers of low resistivity, intermediate resistivity and high resistivity zone. The low resistivity zone is the uncompacted soil which provide an unstable foundation for the building while intermediate and high resistivity zone representing the fairly compacted to compacted soil which provide stable foundations for the buildings. The presence of clayey materials and oversaturated soil around the central part of the campus is the cause of the uneven ground settlement underneath these buildings causing the apparent cracks on some superstructures. The foundation of structures and buildings should be strengthened by mixing of the soil with gravels to enhance stability. Proper electrical resistivity survey and soil penetration test on the soil should be carried out prior to construction of buildings in the campus.

KEYWORDS

Resistivity tomography, Dipole-dipole, Weathered migmatite, Uncompacted soil, Building foundation

1. INTRODUCTION

The search for mineral resources has forced men to dig well and mineshaft which sometimes end fruitlessly. Digging well for subsurface logging to get the information on the different soil layer can be very stressful and time consuming. It is reported that digging is a wild cat activity while surface geophysics methods provide a means of proving the subsurface by means of indirect conductivity surveying of the region which will save time and energy and unnecessary cost of digging non-destructive methods to identify subsurface irregularities without resorting to invasive excavation (Oritsejojolonesan and Sale, 2011).

Geophysics employs the use of non-destructive methods to identify subsurface anamalies without resorting to invasive excavation (Baker, 1993). Non-Destructive Testing (NDT) is the evolution of a mineral's properties, a component's characteristics, or a system's qualities without inflicting harm. (Louis, 1995). Geophysical investigation is one of the methods used in probing the soil/subsoil and subsurface for any engineering construction activities. Geophysical methods are capable of precisely mapping depth to bedrock, bedrock petrography and architecture, depth to the ground water table as well as the lateral and vertical inhomogeneity of sub-soil properties at geotechnical sites. The resolution of the Geophysical data can provide additional insights into the subsurface geology and the cause of foundation failures.

The deduced soil characteristics are used as primary information to determine the suitability of the site for the proposed structure. If this crucial step is omitted, concealed geological features within the subsurface may precipitate excessive total or differential settlement leading to failure or collapse of civil structure. Geophysical method has been found useful in pre and post-construction geotechnical investigation which include the gravity, the electrical resistivity and the seismic refraction method including the Ground Penetration Radar (GPR) (Roth et al., 2002; Fatoba and Salami, 2004; Olurumfemi et al., 2005; Akintorinwa et al., 2011; Salami et al., 2012).

Electrical Resistivity Tomography (ERT) is one of the most popular geophysical tools for near-surface characterization. This is perhaps based on its speed of data acquisition, cost effectiveness and proxy to the spatial and temporal variability of many other subsurface physico-chemical properties such as soil type, porosity, moisture content, clay content and mineralogy, soil water content, organic matter content and bulk density. Clay content for instance can affect the soil strength, porosity and ultimately the conductivity (or resistivity) of the soil matrix in various degree. The iron exchange property of clay lithology forms a mobile cloud of ions around each clay particle, which then expedite the flow of electrical current within the clay matrix, therefore, in fine grained soil like clay, the value of the electrical resistivity is usually lower than expected on the basis of chemical analysis of water and some extracted semiconductors elements from soil (Coseanza et al., 2006; Anderson et al., 2008; Onivefu,

Quick Response Code	Access this article online	
	Website: www.myjgeosc.com	**DOI:** 10.26480/mjg.01.2024.59.75

Cite The Article: Abdulbariu Ibrahim, Jafaru Nasiru, Mu'awiya Baba Aminu, Ayinla Habeeb Ayoola, Mojeed Olaniyi Fasasi, Yinka Benjamin Oluwadiya (2024). Utilising 2-D Resistivity Imaging Tomography in Investigating Structural Failure in Some Buildings in Adankolo Campus of Federal University Lokoja, Nigerian North Central Area. *Malaysian Journal of Geosciences, 8(1): 59-75.*

2023; Onivefu et al., 2024).

Generally, the ERT technique has proven to be non-destructive, minimally invasive and has been applied to various subsurface characterization problems involving groundwater exploration, engineering site investigation, landfill and solute transport delineation, determination of compaction and soil horizon thickness, archaeological prospecting, and assessment of both soil hydrological properties and foundation instability (Cardarelli et al., 2007; Wisen et al., 2008; Oyeyemi et al., 2016; Aizebeokhai and Onyeyemi, 2015; Aizebeokhai et al., 2016). With Vertical Electrical Sounding (VES), only the different layer and the depth of the layers can be delineated using ID program like IPI2WIN, IX1D and WINresist Computer softwares (Changde et al., 2022; Ibrahim et al., 20224; Andarawus et al., 2022; Aizebeokhai et al., 2016). With ERT a more accurate subsurface model can be produced where resistivity changes in the vertical and horizontal direction.

2. Materials and Methods

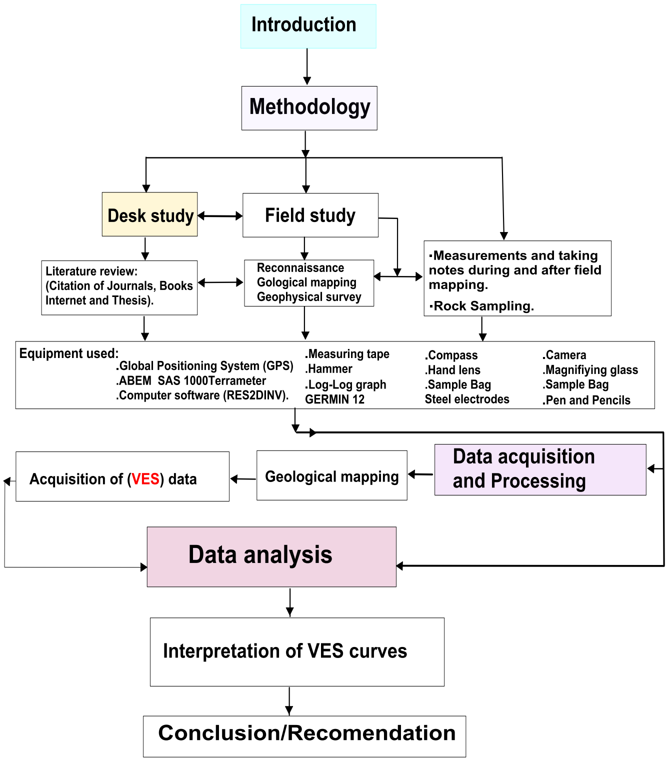

Figure 1: Workflow chart used for this research, (Modified after Abdulbariu et al., 2023; Aminu et al., 2022b).

2.1 Materials

The main equipments employed were the terrameter, a rechargeable battery, reeling cables, Steel electrodes, GERMIN 12, Global Positioning System (GPS), Hammers, Camera, BallPen/Pencil and recording Sheet

Plate 1: Material set up for the ERT survey.

2.2 Method

2.2.1 Electrical Resistivity Method

Electrical Surveys in Geophysics is the revelation of subsurface response yielded by electrical current flow in the subsurface. It is used to study the subsurface resistivity assessment underneath the research area. In a nut shell, the electric current is place into the terrain, and the resulting voltage discrepancies are measured at the surface of the earth. True resistivity of the subsurface can be assessed from this voltage measurement. Anomalous conditions or inhomogeneity in the subsurface, including comparatively conducting or resistive zones, are deduced from the fact that they turn the current and pervert surface potential readings. The content, porosity and degree of water saturation in the rock impact the subsurface current distribution.

It has been adopted in hydrogeological, mining, and geotechnical survey, and for environmental study. Currently, a number of scientific disciplines are quite interested in studying urban environments. Urban environments are changing as a result of human activities such urbanization, carbon emissions, and biodiversity changes. This emphasizes the significance of continuous environmental assessment to protect the health and livability of urban residents (Mudele et al., 2020; Mudele et al., 2021; Onivefu, 2023; Onivefu et al., 2024).

Some elemental theories of the resistivity method are that Electrical resistivity is a degree of how a material contends a stabile electrical current flow. The electrical resistivity of a cylindrical sampling of length L (m) with a uniform cross-section area A (m^2). having resistance R amidst the end faces (as shown in figure 1), is provided by:

$$\boldsymbol{\rho a} = \frac{RA}{L} \tag{1}$$

The unit of resistivity $\boldsymbol{\rho}$ is ohm-meter (Ωm). The resistance R is given in terms of the electric potential $\boldsymbol{V}$ applied across the ends of the cylinder and the resultant current $\boldsymbol{I}$ flowing through it by Ohm's law.

$$R = \frac{V}{I} \tag{2}$$

The units of ***R***, ***V***, and ***I*** are ohms (Ω), volts (***V***), and amperes (***A***) respectively

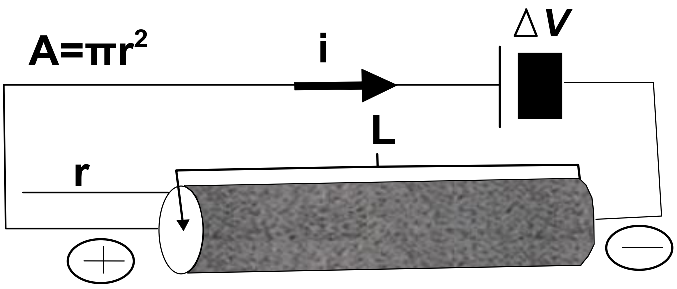

Figure 2: Current passing through a cylindrical body

Geophysical resistivity surveys are based on Ohm's law, an essential physical principle that regulates ground current flow. Ohm's law may be expressed as the following vector:

$$J = \boldsymbol{E}\sigma \tag{3}$$

When J is the current density, E is the electric field intensity, and σ is the electrical conductivity—measured in siemens/m or mholm—the reciprocal of resistivity is expressed as:

$$\rho(\sigma = \frac{1}{\rho})$$

In practice the electric potential V is measured. The relationship between V and E is given by:

$$E = -\text{grad}\, V \tag{4}$$

Adding the two equations above, we obtain:

$$J = -\sigma\, \text{grad}\, V \tag{5}$$

The easiest approach to the theoretical study of the current flow in the ground is to take in to account the first case of a homogenous Isotropic subsurface and a single point current source on the ground surface as illustrated in figure 2.

In this instance, the current emanates radially away from the source. The equipotential surfaces take on a hemispherical for, with the current flow perpendicular within the equipotential surface.

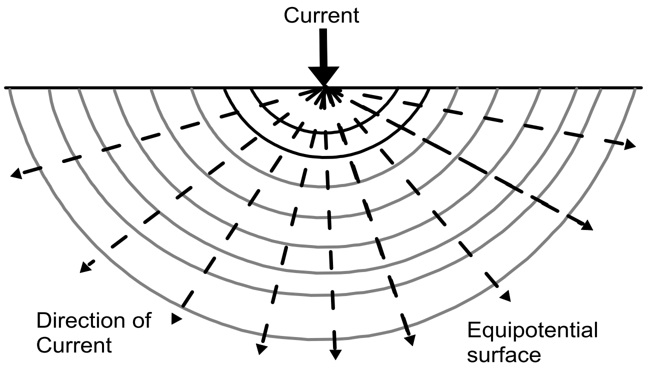

Figure 3: Flow of current in A Homogeneous Isotropic subsurface

At some distance r from the current source, the hemispherical shell has surface area $2\pi r^2$, so the current density J is:

$$J = \frac{I}{2\pi r^2} \tag{6}$$

Since $\rho = \frac{1}{\sigma}$ and using $J = \frac{I}{2\pi r^2}$ then equation $J = -\sigma grad\ V$ can be written as:

$$\frac{I}{2\pi r^2} = -\frac{1}{\rho}\frac{\partial v}{\partial r} \tag{7}$$

And

$$-\frac{\partial v}{\partial r} = \frac{\rho I}{2\pi r^2} \tag{8}$$

The potential V at distance r from the current source is given by integrating the above equation, result of which is:

$$V = \int \left(\frac{\rho I}{2\pi r^2}\right) dr = \frac{I\rho}{\pi r^2} \tag{9}$$

This equation provides fundamental relationship for electrical prospecting carried out at the surface of a uniform isotropic earth. Basically, a single electrode, by itself, cannot inject current into half-space; a return electrode is required such that the current flows into the ground via one (source) and exits via the other (sink) electrode (as shown in figure 3) the potential measure at passive electrode P_2 due to current entering and exiting via active electrodes C_1 and C_2 is:

$$V_{P_1} = \frac{I\rho}{2\pi}\left[\frac{1}{r_{c_1P_1}} - \frac{1}{r_{c_2P_1}}\right] \tag{10}$$

The minus sign in the second term of this equation recognized the change in sign of the current at the source and sink electrodes C_1 and C_{21} and where $r_{c_1P_1}$ is the distance between P_1 and C_1 while $r_{c_2P_1}$ is the distance between P_2 a and C_2

In practice a potential difference between two points, rather than an absolute potential, is measured. The potential difference for a four (4) electrodes array is given by:

$$\Delta V = V_{P_1} - V_{P_2} \tag{11}$$

and

$$\Delta V = \frac{I\rho}{2\pi}\left[\frac{1}{r_{c_1P_1}} - \frac{1}{r_{c_2P_1}} - \frac{1}{r_{c_1P_2}} + \frac{1}{r_{c_2P_2}}\right] \tag{12}$$

The resistivity of a half-space is then determined by solving aforementioned equation for ρ which is:

$$\rho = \frac{2\pi}{\Delta V}\left[\frac{1}{r_{c_1P_1}} - \frac{1}{r_{c_2P_1}} - \frac{1}{r_{c_1P_2}} + \frac{1}{r_{c_2P_2}}\right] \tag{13}$$

And

$$\rho = k\frac{\Delta V}{I} \tag{14}$$

k is called the *geometric factor* which depends on the specific configuration of current and potential electrodes.

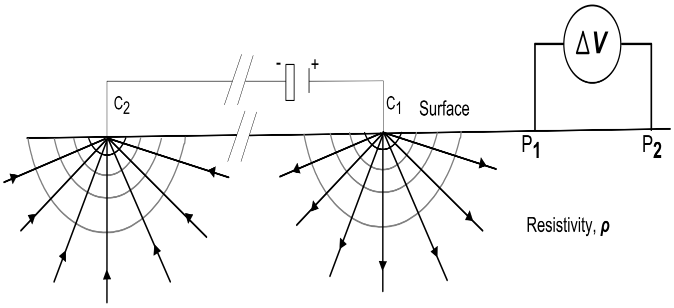

Figure 4: Flow of current in half space

2.2.2 Electrode Configurations/Array

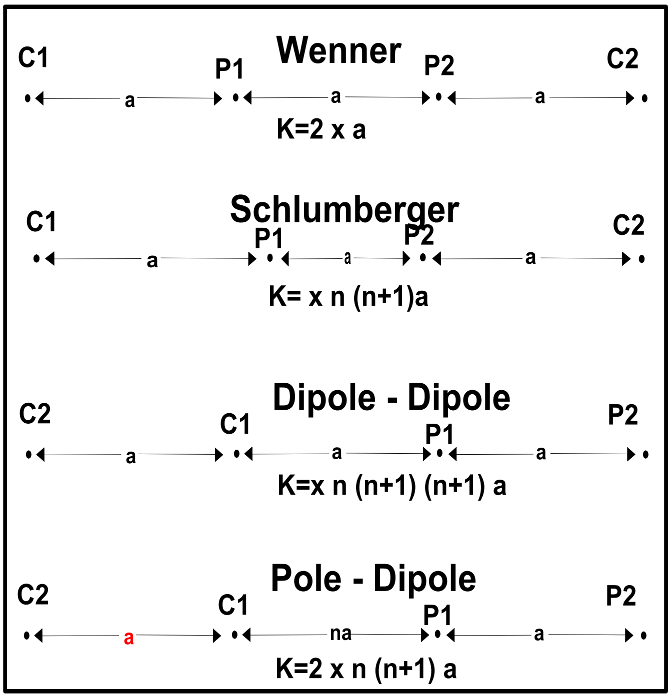

Figure 5: Four common electrode array/configuration

Common arrays used in resistivity surveys and their geometric factors. Note that the dipole-dipole, pole-dipole and schlumberger arrays have two parameters, the dipole length "a" and the dipole separation factor "n" while the "n" factor is commonly an integer value; non-integer value can also be used. k is the geometric factor.

The four-electrode configuration's real resistivity, which would be determined from potential measurements over a homogeneous half-space, is given by equation (xiii).

The resulting resistivity is constant and independent of the configuration of the electrodes on the surface as well.

For an inhomogeneous earth the resistivity ρ computed from the equation will change according to the geometric arrangement of the electrodes or on the horizontal position of the array.

The resistivity obtained, for an inhomogeneous surface is, accordingly, properly viewed as an apparent resistivity, denoted by:

$$\rho_a = k\frac{\Delta V}{I} \tag{15}$$

The apparent resistivity should not be considered as some kind of a specially averaged resistivity of the homogeneous sub surface formation. It is the resistivity that the potential readings would attribute to the ground if it were homogeneous. The network between the apparent resistivity and the true resistivity is a complex relationship. To ascertain the true subterranean resistivity from the measured apparent resistivity values is the" *inversion*" problem or "*inverse modelling* ".

2.2.3 Inverse Modelling

Calculating the resistivity distribution that is 'consistent' with the observed (measured) resistances.

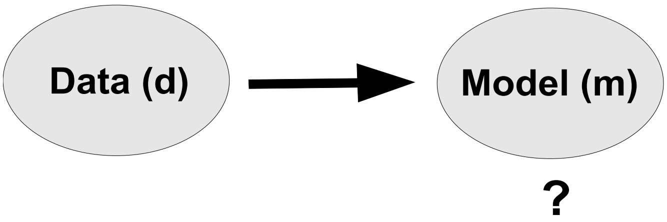

Figure 6: Inverse model

2.2.4 Forward Modelling

Calculating the resistance that would theoretically be 'measured' for a given resistivity distribution

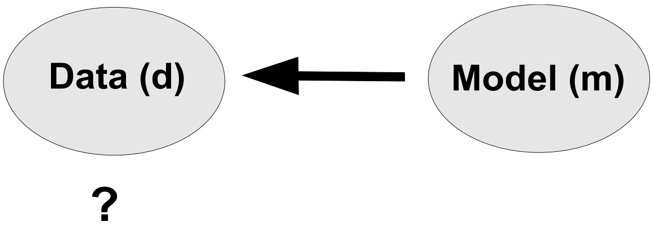

Figure 7: Forward model

2.3 Electrical Resistivity of Rocks, Soils, And Minerals

Igneous and Metamorphic Rocks: generally, have high resistivity values. The resistivity of these rocks is highly dependent on the degree of fracturing, and the percentage of the fractures packed with ground water. Thereby, a given rock type can have an extensive value of resistivity, from about 1000 to 10 million ohm-m, depending upon on even it is wet or dry. This characteristic is vital in the identification of fracture zones and other weathering characteristics, such as in engineering and groundwater explorations.

Sedimentary Rocks: which are commonly more porous and have more water content, normally have less resistivity values compared to igneous and metamorphic rocks. The resistivity values range from 10 to about 10000 ohm-m, with most values below 1000 ohm-m. The resistivity values are largely dependent on the porosity of the rocks, and the salinity of the contained water. Unconsolidated Sediments: generally, have even lower resistivity values than sedimentary rocks, with values ranging from about 10 to less than 1000 ohm-m. The resistivity value is dependent on the porosity (assuming all the pores are saturated) as well as the clay content. Clayey soil normally has a lower resistivity value than sandy soil. Note the overlap in the resistivity values of the different classes of rocks and soils. This is because the resistivity of a particular rock or soil sample depends on a number of factors such as the porosity, the degree of water saturation and the concentration of dissolved salts.

Groundwater has resistivity values vary from l0 to 100 ohm-m depending on the concentration of dissolved salts. Note the low resistivity (about 0.2 ohm-m) of seawater due to the relatively high salt content. This makes the resistivity method an ideal technique for mapping the saline and fresh water Interface in coastal areas.

Metallic Sulfides: Metallic sulfides (such as pyrrhotite, galena and pyrite) have typically low resistivity values of less than 1 ohm-m. Note that the resistivity value of a particular ore body can differ greatly from the resistivity of the individual crystals, other factors, such as the nature of the ore body (massive or disseminated) have a significant effect. Most oxides, such as hematite, do not have a significantly low resistivity value, except magnetite.

Industrial Contaminants: Metals, such as iron, have extremely low resistivity values. Chemicals that are strong electrolytes, such as potassium chloride and sodium chloride, can greatly reduce the resistivity of ground water to less than 1 ohm-m even at fairly low concentrations. Hydrocarbons, such as xylene, typically have very high resistivity values. However, in practice the percentage of hydrocarbons in a rock or soil is usually quite small, and might not have a significant effect on the bulk resistivity.

Archie's law gives the relationship between the resistivity of a porous rock and the fluid saturation factor.

$$\boldsymbol{\rho = a\emptyset^{-m} S_{w^{-n}} \rho_w}$$

Where $\boldsymbol{\rho}$ = resistivity of the rock, $\boldsymbol{\rho_w}$ resistivity of the pore water, S_w= (volume of water in pores)/(total volume of pores)., m= cementation factor, -2 for well-cemented formation ., ~≤ 1.5 for moderate to poorly cemented formations., $n =$ saturation exponent, normally = 2., a = coefficient of saturation, =between 0.6-2., Ø fractional porosity.

It is applicable for certain types of rocks and sediments, particularly those that have a low clay content. The electrical conduction is assumed to be through the fluids filling the pores of the rock.

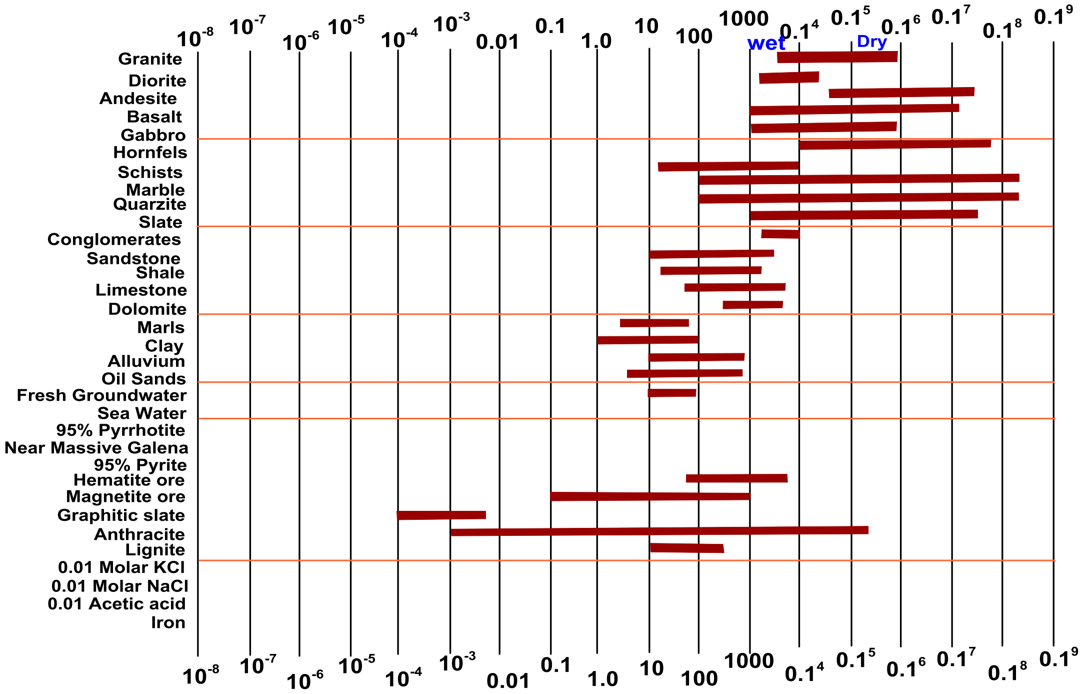

Figure 8: Resistivity values of common rocks, Soil materials and chemicals (Keller and Friscknecht 1966).

2.4 Data Acquisition

The ABEM SAS 1000 terrameter was used for the survey along the transverse along with four (4) cables and four stakes for the electrodes. The electrodes spacing was 5m and Dipole-Dipole array was used. The "*role along*" technique was used which involves removing the electrodes after a data for the point is obtained and placing them again on another point to get data for another point and so on. The (n) factor is increased by

1 to penetrate to a deeper depth after a data point is collected to save time and energy instead of using *n*=1 for the entire survey line before starting over with *n*=2; extending only the potential electrode for a survey line.

Using the dipole-dipole array, the electrodes were positioned symmetrically along a straight line, with two current electrodes placed before the potential electrodes, Both the current and potential electrode positions were aligned using constant electrode spacing of 5m (i.e. a = 5m) tor long profiles and 3(a = 3m) for shorter profiles, The space between the current electrodes and the potential electrode increases by 5m for a constant electrode spacing (a) of 5m and by 3m for a constant electrode spacing (a) of 3m. Points where the electrodes meet the pavements and road were omitted and assigned a resistivity value of infinity (∞) and areas where the profile terminated and where electrode configuration couldn't be aligned completely were dashed to indicate no data.

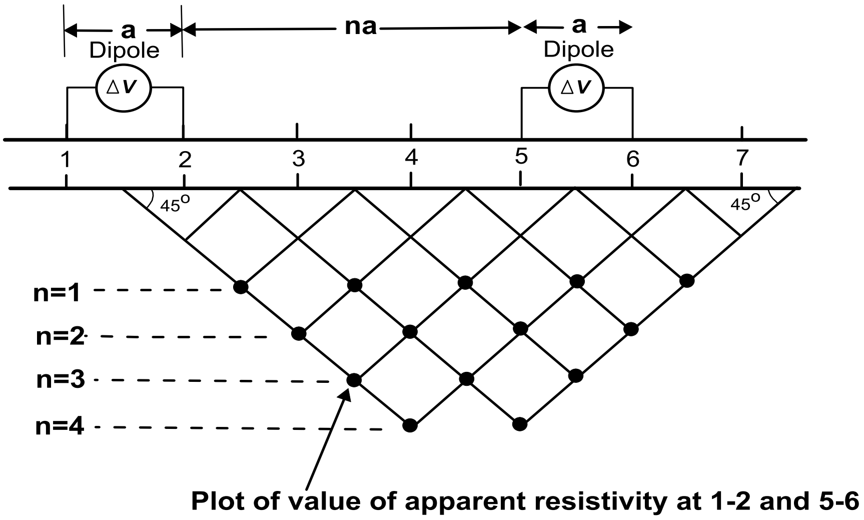

Figure 9: Dipole-Dipole 2-D Resistivity Data Collection for a Pseudosection.

Method of plotting dipole-dipole apparent resistivity data in a Pseudosection. n represent the relative spacing between the current and potential dipoles.

2.5 Electrical Resistivity Tomography Modelling

Two-dimensional ERT investigations were conducted using an ABEM Terrameter (SAS 1000) along the two survey traverses E-W and N-S, The ERT lines E-W and N-S have a minimum length of 34m (ERT 3) and maximum length of l15m were acquired using a Dipole-dipole array with minimum and maximum electrode spacing of 0.3m and 5.0m respectively, and maximum current and potential electrode spacing of 25,0m (n =5 for a= 5) resulting in 5 depth levels.

A total number of 258 data points (apparent resistivity) were acquired. Data interpretation was based on a 2-D model of the subsurface which consists of a number of rectangular blocks. The observed apparent resistivity data were processed and inverted using RES2DINV code, employing a least squares inversion modeling technique with regularization technique (Loke and Barker, 1996). Various 2D resistivity data was acquired from the study area together with the distance in which the data was taken to produce a 2-D resistivity image for the study area. The data acquired was inverted and gridded by the RES2DINV software to produce a 2-D Electrical Resistivity Tomography (ERT).

Pseudosections are normally used to display apparent resistivity data from a 2-D resistivity survey. A horizontal location is defined as the mid-point of the electrode array used to make a given apparent resistivity measurement. A vertical location is defined to be some distance that is proportional to the separation between the electrodes or estimate depth (pseudo depth) of electrode array used.

For the Dipole-dipole array, for example, apparent resistivity data are plotted at the intersection of the two lines drawn at a 45^0 angle to the horizon from the center of the current (C_1-C_2) and the potential (P_1-P_2) dipole pairs.

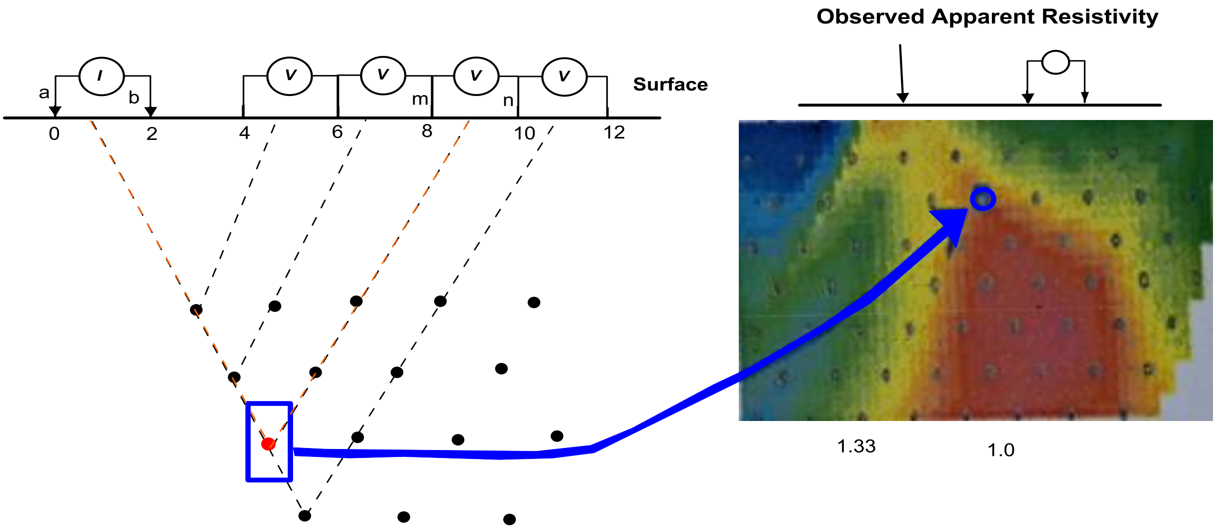

Figure 10: Dipole-Dipole 2-D Resistivity Data Converted to a Pseudosection

2.6 Sounding Locations

The site layout is shown in plate 2 where the building surveyed is enclosed in blue rectangles and the survey line represented with red arrows. Figure 11 shows the sketch of the ERT lines. The buildings surveyed are the library, the large lecture rooms (4&5), the laboratories (computer., geography, post-graduate economics), sport center, food canteen and the university health center (pharmacy and clinic). Plate 3 shows the major cracks on the PG Economics Lab Block while plate 3 shows the major cracks on the LLR4 Block. A predetermined survey line or profile line runs straight along the side of the buildings under investigation and the resistivity data of the sections recorded on the field resistivity data sheet.

Cite The Article: Abdulbariu Ibrahim, Jafaru Nasiru, Mu'awiya Baba Aminu, Ayinla Habeeb Ayoola, Mojeed Olaniyi Fasasi , Yinka Benjamin Oluwadiya (2024). Utilising 2-D Resistivity Imaging Tomography in Investigating Structural Failure in Some Buildings in Adankolo Campus of Federal University Lokoja, Nigerian North Central Area. *Malaysian Journal of Geosciences, 8(1): 59-75.*

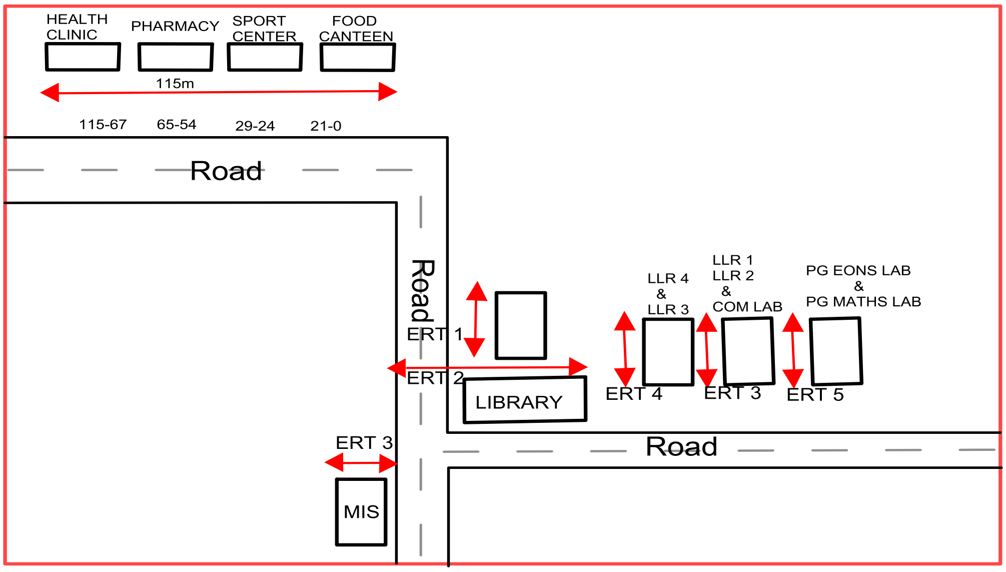

Figure 11: sketch showing ERT in the Campus

Plate 2: Cracks on the PG Economics Lab

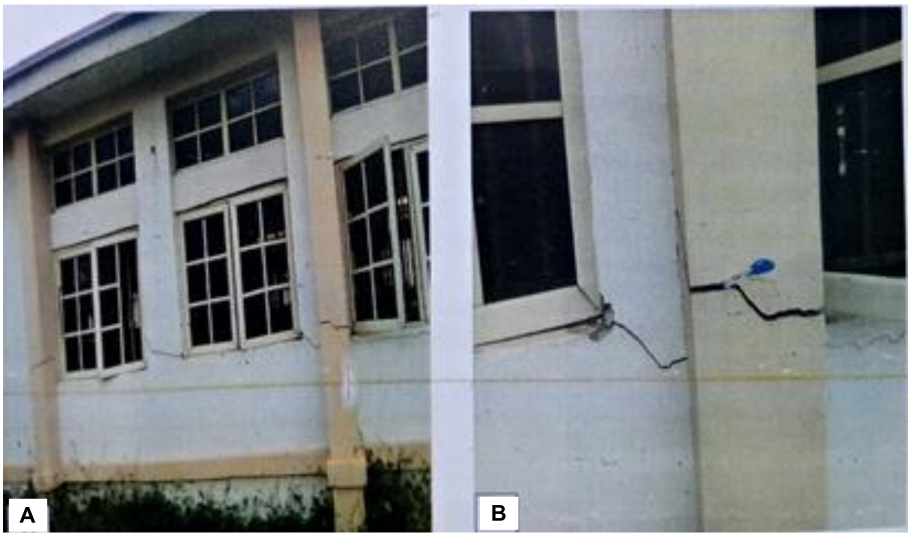

Plate 3: Cracks on the LLR4 Block

3. Results

Table 1 to 7 shows the result of the 2D survey along a traverse for the investigated buildings. Figure 4.2 to 4.8 show the 2D electrical resistivity tomography (ERT) for the 10-building site investigated where the ERT profile run along the building structure. ERT 1, ERT 2, ERT 3, ERT 4 ERT 5, ERT 6 represent the survey line along the geography lab, Library, MIS, LLR4, Computer lab, PG Economics Lab respectively while the ERT 7 represents survey line along the Sport Centre, food Canteen, Pharmacy and Health Clinic blocks. The figures show the measured apparent resistivity, calculated apparent resistivity and the inverse model resistivity section produced after optimization to reduce the root-mean-square error between them. The inverse model resistivity sections are displayed as functions of resistivity in Ohm-meter versus soil depth in meters and are inferred from the processed pseudo-section. Resistivity.

Table 1: Dipole-Dipole Resistivity Data Sheet along the transverse E-W for ERT 1 (Geography Lab)							
ELECTRODE POSITIONING					RESISTIVITY PARAMETER		
N	**C_1**	**C_2**	**P_1**	**P_2**	**K**	**R(Ω)**	**ρa (Ω)**
1	0	1	2	3	94.2478		7.12
2			3	4	376.9911		9.63
3			4	5	942.4778		11.01
4			5	6	1884.956		17,16
5			6	7	3298.672		22.68
1	1	2	3	4	94.2478		8.22
2			4	5	376.991		7.68
3			5	6	942.4778		6.39
4			6	7	1884.956		13.17
5			7	8	3298.672		10.76
1	2	3	4	5	94.2478		7.4
2			5	6	376.9911		11.35
3			6	7	942.47.778		13.71
4			7	8	1884.956		13.77
5			8	9	3298.672		11.82
1	3	4	5	6	94.2478		8.65
2			6	7	376.9911		8.17
3			7	8	942.4778		8
4			8	9	1884.956		6.72
5			9	10	3298.672		1277
1	4	5	6	7	94.2478		13.07
2			7	8	376.9911		8.98
3			8	9	942.4778		8.02
4			9	10	1884.956		11.6
5			10	11	3298.672		8.91
1	5	6	7	8	94.2478		19.61
2			8	9	376.9911		10.62
3			9	10	942.4778		11.28
4			10	11	1884.956		9.39
5			11	12	3298.672		----
1	6	7	8	9	94.2478		10.55
2			9	10	376.9911		12.75
3			10	11	942.4778		10.22
4			11	12	1884.956		------
5			12	13	3298.672		-------
1	7	8	9	10	94.2478		13.63
2			10	11	376.9911		8.19
3			11	12	942.4778		------
4			12	13	1884.956		------
5			13	14	3298.672		------

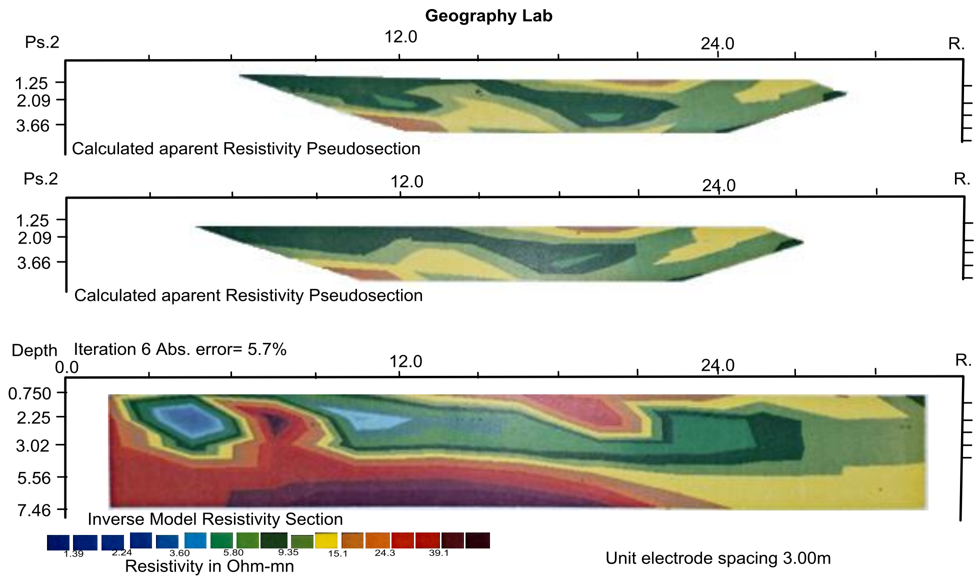

Figure 12: 2-D Resistivity image for profile ERT 1

Cite The Article: Abdulbariu Ibrahim, Jafaru Nasiru, Mu'awiya Baba Aminu, Ayinla Habeeb Ayoola, Mojeed Olaniyi Fasasi , Yinka Benjamin Oluwadiya (2024). Utilising 2-D Resistivity Imaging Tomography in Investigating Structural Failure in Some Buildings in Adankolo Campus of Federal University Lokoja, Nigerian North Central Area. *Malaysian Journal of Geosciences, 8(1): 59-75.*

Figure 12 shows the result for the ERT 1 profile along the geography lab. Three resistive zones were observed. Low resistive zone (deep blue-light blue), intermediate resistive zone (green- brown) and high resistive zone (orange-purple). Lowest resistivity values for this profile in range of <3.6m is observed at approximately 3.0m to 6.0m surface distance and 0.75m to 3.82m depth. Low resistivity of2.24Ωm to3.6Ωm is observed between 9.0m to 6m surface distance and 0.75mto 3.82 depth. The zone of low resistivity is deduced to indicate the presence of waste water from the small soak away behind the buildings. Intermediate resistivity zone of 15.3Ωm to 24.3Ωm is observed along the entire length of the profile. The highest resistivity values of 24.3Ωm to 39.1Ωm were observed at the depth of approximately 3.82m to 7.46m and stretches laterally for clayey/lateritic soil. The foundation present here is considered to be on top of a moderately approximately 30m. This zone is deduced to be moderately compacted and represents highly competent layer and no structural defect was observed on the building.

Table 2: Dipole-Dipole Resistivity Data Sheet along the transverse E-W for ERT 2 (Library block)

ELECTRODE POSITIONING					RESISTIVITY PARAMETER		
N	C_1	C_2	P_1	P_2	K	R(Ω)	ρa (Ω)
1	0	1	2	3	94.2478		7.18
2			3	4	376.9911		104.86
3			4	5	942.4778		5.64
4			5	6	1884.956		32.62
5			6	7	3298.672		22.08
1	1	2	3	4	94.2478		7.03
2			4	5	376.9911		7.18
3			5	6	942.4778		8.39
4			6	7	1884.956		9.98
5			7	8	3298.672		∞
1	2	3	4	5	94.2478		11.36
2			5	6	376.9911		9.34
3			6	7	942.47778		24.24
4			7	8	1884.956		∞
5			8	9	3298.672		∞
1	3	4	5	6	94.2478		10.95
2			6	7	376.9911		9.85
3			7	8	942.4778		∞
4			8	9	1884.956		∞
5			9	10	3298.672		∞
1	4	5	6	7	94.2478		10.96
2			7	8	376.9911		∞
3			8	9	942.4778		∞
4			9	10	1884.956		∞
5			10	11	3298.672		∞
1	5	6	7	8	94.2478		∞
2			8	9	376.9911		∞
3			9	10	942.4778		∞
4			10	11	1884.956		85.57
5			11	12	3298.672		4.71
1	6	7	8	9	94.2478		∞
2			9	10	376.9911		∞
3			10	11	942.4778		1.94
4			11	12	1884.956		5.88
5			12	13	3298.672		8.38

Figure 13 shows the result for the ERT 2 profile along the library block. Data couldn't be taken for some point along the traverse in areas the electrodes were to be staked on a pavement or road and a value of infinity (∞) is assigned (as Shown in table 2). Because the RES2DINV software cannot process the infinity sign, data for the point was left blank when preparing the data file for the software. The low resistivity region to the left at surface distance 33m to 63m at depth 1.25m to 12.4m represents the tar road adjacent to the campus Library, Low resistivity zone of <3.56Ωm is observed at surface distance of 20m to 25m at depth 1.25m to 6.38m. This is most likely an interference from a soakaway beside the building. An Intermediate resistivity zone of 18.0Ωm to 31Ωm is observed at surface distance 0m to 35m at depth 6.38m to 12.4m also at surface distance 23m to 30m at depth 1.25m. this zone is detected to be moderately compacted and the foundation is considered to be situated on a fairy competent soil which can be inferred to be made of highly weathered basement.

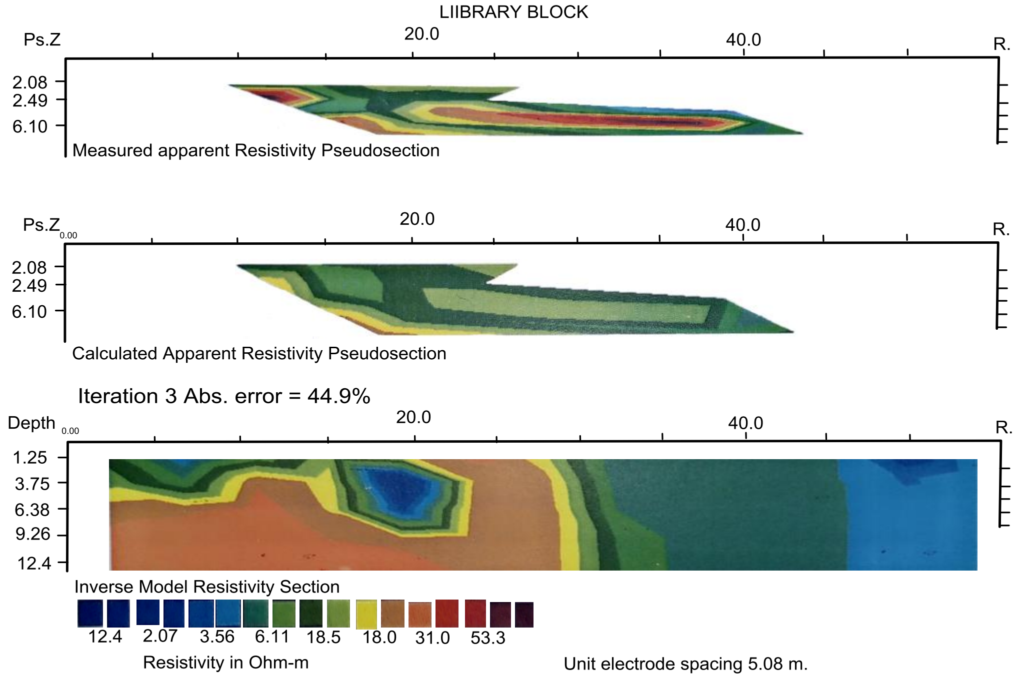

Figure 13: 2-D Resistivity image for profile ERT 2

Table 3: Dipole-Dipole Resistivity Data Sheet for ERT 3 (MIS block)							
ELECTRODE POSITIONING					RESISTIVITY PARAMETER		
N	C_1	C_2	P_1	P_2	K	R(Ω)	ρa (Ω)
1	0	1	2	3	94.2478		10.13
2			3	4	376.9911		10.79
3			4	5	942.4778		13.08
4			5	6	1884.956		9.37
5			6	7	3298.672		9.13
1	1	2	3	4	94.2478		7.82
2			4	5	376.9911		5.74
3			5	6	942.4778		5.02
4			6	7	1884.956		5.3
5			7	8	3298.672		4.87
1	2	3	4	5	94.2478		8.45
2			5	6	376.9911		5.34
3			6	7	942.47.778		4.91
4			7	8	1884.956		4.88
5			8	9	3298.672		---
1	3	4	5	6	94.2478		13.25
2			6	7	376.9911		7.84
3			7	8	942.4778		5.52
4			8	9	1884.956		-----
5			9	10	3298.672		------
1	4	5	6	7	94.2478		9.63
2			7	8	376.9911		9.51
3			8	9	942.4778		------
4			9	10	1884.956		-----
5			10	11	3298.672		------
1	5	6	7	8	94.2478		9.06
2			8	9	376.9911		----
3			9	10	942.4778		----
4			10	11	1884.956		----
5			11	12	3298.672		----

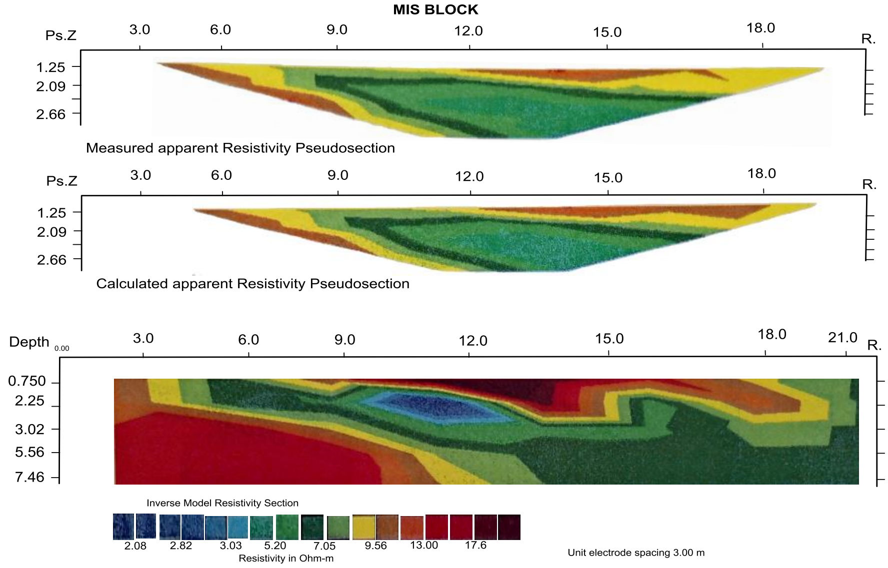

Figure 14: 2-D Resistivity image for profile ERT 3

Figure 14 shows the results of the ERT 3 profile along the MIS block. Three resistivity zone exist with the intermediate and high resistivity zone occurring on a wider extend. The low resistivity zone isolated as surface distance of approximately 9m to 12m at a depth of 0.25Ωm to 3.82Ωm with resistivity range of 2.82Ωm to 3.83Ωm. This is believed be an interference from the soak away waste water dump adjacent to the profile line. The intermediate zone of resistivity ranges from 5.20Ωm to 9.65Ωm stretches along the entire length of the profile and depth with varying thickness. Two high resistivity zones are present both at the surface and bottom with resistivity range of 13.0Ωm to 17.6Ωm at distance 6m to 21m and 0m to 10m respectively. Resistivity range of <17.6Ωm is observed for this area and the lithology is inferred to be clayer/lateritic.

Table 4: Dipole-Dipole Resistivity Data Sheet for ERT 4 (LLR 4 Block).

ELECTRODE POSITIONING					RESISTIVITY PARAMETER		
N	C_1	C_2	P_1	P_2	K	R(Ω)	$\rho a(\Omega)$
1	0	1	2	3	94.2478		12.55
2			3	4	376.9911		16.43
3			4	5	942.4778		15.06
4			5	6	1884.956		8.60
5			6	7	3298.672		19.09
1	1	2	3	4	94.2478		117.99
2			4	5	376.9911		6.41
3			5	6	942.4778		12.75
4			6	7	1884.956		12.50
5			7	8	3298.672		14.98
1	2	3	4	5	94.2478		8.24
2			5	6	376.9911		9.61
3			6	7	942.47778		11.46
4			7	8	1884.956		12.17
5			8	9	3298.672		290.16
1	3	4	5	6	94.2478		6.36
2			6	7	376.9911		8.04
3			7	8	942.4778		11.73
4			8	9	1884.956		11.76
5			9	10	3298.672		14.48
1	4	5	6	7	94.2478		8.14
2			7	8	376.9911		10.28
3			8	9	942.4778		11.84
4			9	10	1884.956		14.21
5			10	11	3298.672		-----
1	5	6	7	8	94.2478		8.64
2			8	9	376.9911		9.6
3			9	10	942.4778		11.75
4			10	11	1884.956		----
5			11	12	3298.672		----
1	6	7	8	9	94.2478		8.68
2			9	10	376.9911		9.63
3			10	11	942.4778		-----
4			11	12	1884.956		------
5			12	13	3298.672		-------
1	7	8	9	10	94.2478		9.91
2			10	11	376.9911		------
3			11	12	942.4778		------
4			12	13	1884.956		------
5			13	14	3298.672		------

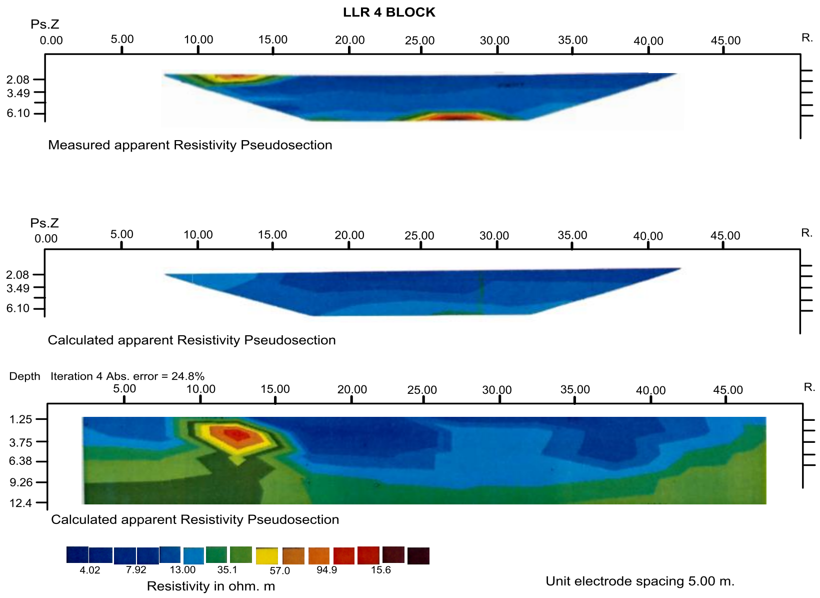

Figure 15: 2-D Resistivity Tomogram for ERT 4

Figure 15 shows the result for the ERT4 profile along the LLR4 block. This pseudo-section shows the largest stretch of the low resistivity zone in range of 4.82Ωm to 13.0Ωm which occur along the total length of the profile and extends from the surface to a depth of 9.26m. This low resistivity Zone is indicative of highly porous and structurally weak soil and is characterized as incompetent which explains why the LLR4 block experience the highest number of cracks, some deep enough that a pen can be inserted in between the cracks without force (as shown in plate 3). Underlining the low resistivity zone is a zone of intermediate resistivity of 21.4Ωm to 35.1Ωm. This zone is deduced to be more compacted than the overlying layer. A pocket of high resistivity zone of 94.9Ωm to 156Ωm is isolated at approximately distance 11m to 14m at depth 3.75m. This is deduced to be a buried rock in the area. Foundation material here is generally considered to be incompetent especially to a depth of 9.26m as very low resistivity is observed.

Table 5: Dipole-Dipole Resistivity Data Sheet for ERT 5 (Computer Lab).

ELECTRODE POSITIONING					RESISTIVITY PARAMETER		
N	C_1	C_2	P_1	P_2	K	R(Ω)	$\rho a(\Omega)$
1	0	1	2	3	94.2478		12.78
2			3	4	376.9911		14.59
3			4	5	942.4778		18.21
4			5	6	1884.956		20.58
5			6	7	3298.672		24.54
1	1	2	3	4	94.2478		12.97
2			4	5	376.9911		14.27
3			5	6	942.4778		15.72
4			6	7	1884.956		17.31
5			7	8	3298.672		16.24
1	2	3	4	5	94.2478		12.39
2			5	6	376.9911		14.93
3			6	7	942.47778		19.66
4			7	8	1884.956		12.22
5			8	9	3298.672		20.69
1	3	4	5	6	94.2478		11.79
2			6	7	376.9911		13.22
3			7	8	942.4778		17.26
4			8	9	1884.956		20.59
5			9	10	3298.672		20.1
1	4	5	6	7	94.2478		10.98
2			7	8	376.9911		10.58
3			8	9	942.4778		12. 43
4			9	10	1884.956		16.97
5			10	11	3298.672		-----
1	5	6	7	8	94.2478		9.69
2			8	9	376.9911		10.11
3			9	10	942.4778		12.13
4			10	11	1884.956		----
5			11	12	3298.672		----
1	6	7	8	9	94.2478		12.31
2			9	10	376.9911		5.69
3			10	11	942.4778		-----
4			11	12	1884.956		------
5			12	13	3298.672		-------
1	7	8	9	10	94.2478		6.51
2			10	11	376.9911		------
3			11	12	942.4778		------
4			12	13	1884.956		------
5			13	14	3298.672		------

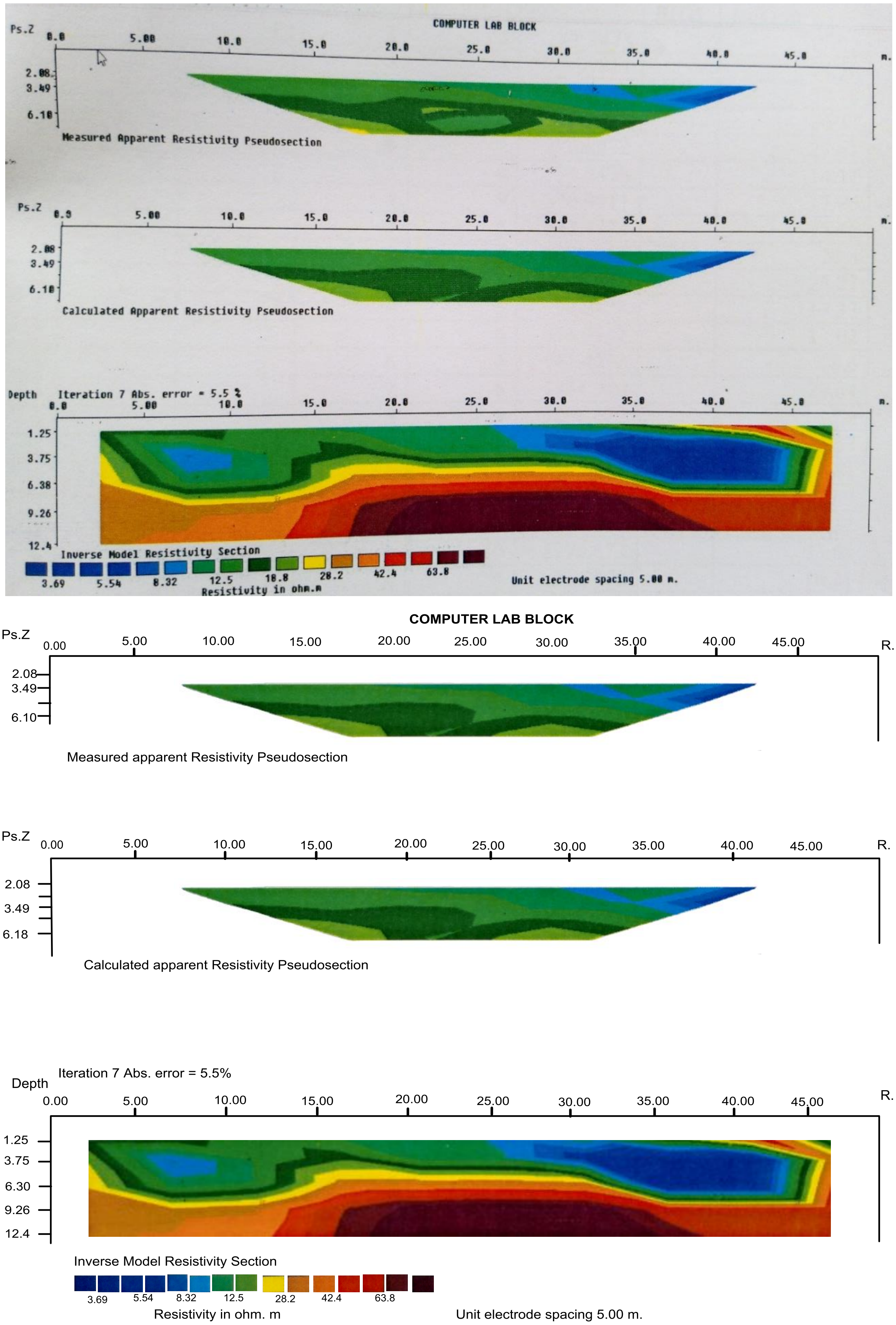

Figure 16: 2-D Resistivity Tomogram for profile ERT 5

Figure 16 shows the result for the ERT 5 profile along the computer lab block. Lowest resistivity of <8.32Ωm is observed at surface distance 5m to 10m at depth 1.25m to 6.30m. This zone indicates the presence of pollutants from the small soakaway at the back of the SIWES Unit Office. A very low resistivity zone of< 5.54Ωm is observed at surface distance 30m to 45m. this is indicative of the presence of un-compacted soil. Intermediate resistivity zone of 12.5Ωm to20.2Ωm is observed at surface distance of 3m to 15m at depth 3.75m. This zone indicates the presence of clayey/ lateritic soil. At surface distance 13m to 48m and depth 9.26m to 12.4m is a zone of high resistivity of 42.4Ωm to 63,8Ωm. This zone indicates highly weathered basement rock. The foundation soil is considered moderately competent and the low resistivity zones are produced by the effect of waste water pollutants in the soil.

Table 6: Dipole-Dipole Resistivity Data Sheet for ERT 6 (PG Economics Lab).

ELECTRODE POSITIONING					RESISTIVITY PARAMETER		
N	C_1	C_2	P_1	P_2	K	R(Ω)	ρa (Ω)
1	0	1	2	3	94.2478		17.04
2			3	4	376.9911		23.56
3			4	5	942.4778		27.78
4			5	6	1884.956		20.33
5			6	7	3298.672		27.61
1	1	2	3	4	94.2478		14.11
2			4	5	376.9911		17.06
3			5	6	942.4778		15.46
4			6	7	1884.956		20.8
5			7	8	3298.672		25.27
1	2	3	4	5	94.2478		17.33
2			5	6	376.9911		13.02
3			6	7	942.47778		18.6
4			7	8	1884.956		23.84
5			8	9	3298.672		25.6
1	3	4	5	6	94.2478		23.57
2			6	7	376.9911		14.81
3			7	8	942.4778		19.99
4			8	9	1884.956		22.32
5			9	10	3298.672		33.66
1	4	5	6	7	94.2478		16.21
2			7	8	376.9911		14.33
3			8	9	942.4778		14. 43
4			9	10	1884.956		25.06
5			10	11	3298.672		33.35
1	5	6	7	8	94.2478		17.06
2			8	9	376.9911		16.12
3			9	10	942.4778		11.52
4			10	11	1884.956		24.38
5			11	12	3298.672		----
1	6	7	8	9	94.2478		15.57
2			9	10	376.9911		436.44
3			10	11	942.4778		22.03
4			11	12	1884.956		------
5			12	13	3298.672		-------
1	7	8	9	10	94.2478		8.84
2			10	11	376.9911		------
3			11	12	942.4778		21.09
4			12	13	1884.956		------
5			13	14	3298.672		------

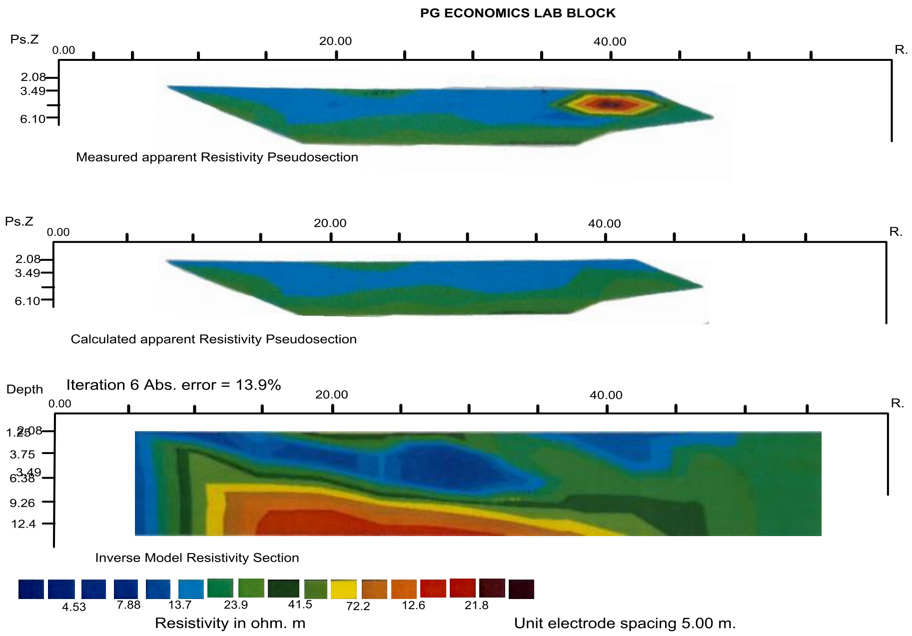

Figure 17: 2-D Resistivity Tomogram for profile ERT 6

Figure 17 shows the result for the ERT 6 profile along the PG Economics Lab. Low resistivity zone exist at distance 3m to 5m and continue downward to a depth of 12.4m. This area on the building experience a large crack and which has been sealed up by filling it with cement. The crack exists to the front and back of the building (as shown in plate 2) The low resistivity zone stretches almost along the entire profile length at a shallow depth of 1.25m to 12.4m. The soil in this region is considered incompetent and is susceptible to collapse. The intermediate resistivity zone of 23.9Ωm to 72.2Ωm occurs from surface distance 5m to 50m at depth of 3.75m to 12.4m. At a depth of 9.23m to 12.4m, there exist a high resistivity zone of 72.2Ωm to 126Ωm which extend laterally from distance 10m to 40m. The intermediate resistivity zone and high resistivity zone indicate a moderately compacted to highly compacted clayey soil

Table 7: Dipole-Dipole Resistivity Data Sheet for ERT 7 (Health clinic, Pharmacy, etc. Sport Center Block).

ELECTRODE POSITIONING					RESISTIVITY PARAMETER		
N	C_1	C_2	P_1	P_2	K	R(Ω)	ρa (Ω)
1	0	0	2	3	94.2478		62.76
2			3	4	376.9911		55.63
3			4	5	942.4778		52.58
4			5	6	1884.956		43.28
5			6	7	3298.672		52.21
1	1	2	3	4	94.2478		57.63
2			4	5	376.9911		52.61
3			5	6	942.4778		55.18
4			6	7	1884.956		68.61
5			7	8	3298.672		71.06
1	2	3	4	5	94.2478		81.44
2			5	6	376.9911		75.23
3			6	7	942.47778		101.56
4			7	8	1884.956		93.54
5			8	9	3298.672		123.27
1	3	4	5	6	94.2478		66.12
2			6	7	376.9911		74.32
3			7	8	942.4778		59.51
4			8	9	1884.956		83.52
5			9	10	3298.672		44.61
1	4	5	6	7	94.2478		98.2
2			7	8	376.9911		56.14
3			8	9	942.4778		64. 37
4			9	10	1884.956		46.22
5			10	11	3298.672		145.18
1	5	6	7	8	94.2478		71.35
2			8	9	376.9911		88.94
3			9	10	942.4778		59.2
4			10	11	1884.956		94.69
5			11	12	3298.672		68.54
1	6	7	8	9	94.2478		90.56
2			9	10	376.9911		67.69
3			10	11	942.4778		148.13
4			11	12	1884.956		130.99
5			12	13	3298.672		60.67
1	7	8	9	10	94.2478		61.6
2			10	11	376.9911		62.94
3			11	12	942.4778		63.15
4			12	13	1884.956		34.13
5			13	14	3298.672		93.3
1	8	9	14	15	94.2478		130.75
2			15	16	376.9911		126.73
3			16	17	942.4778		55.45
4			17	18	1884.956		104.91
5			18	19	3298.672		117.32
1	9	10	19	20	94.2478		95.48
2			20	21	376.9911		52.07
3			21	22	942.4778		64.16
4			22	23	1884.956		206.89

Table 7: Dipole-Dipole Resistivity Data Sheet for ERT 7 (Health clinic, Pharmacy, etc. Sport Center Block).

5			23	24	3298.672		152.94
1	10	11	54	25	94.2478		63.17
2			25	26	376.9911		52.52
3			26	27	942.4778		108.08
4			27	28	1884.956		90.99
5			28	29	3298.672		83.86
1	11	12	29	30	94.2478		85.5
2			30	31	376.9911		141.12
3			31	32	942.4778		157.47
4			32	33	1884.956		157.14
5			33	34	3298.672		48.56
1	12	13	34	35	94.2478		41.39
2			35	36	376.9911		57.62
3			36	37	942.4778		39.92
4			37	38	1884.956		564.62
5			38	39	3298.672		31.41
1	13	14	39	40	94.2478		69.37
2			40	41	376.9911		61.73
3			41	42	942.4778		77.86
4			42	43	1884.956		34.79
5			43	44	3298.672		19.95
1	14	15	44	45	94.2478		78.88
2			45	46	376.9911		77.41
3			46	47	942.4778		37.54
4			47	48	1884.956		28.8
5			48	49	3298.672		178.51
1	15	16	49	50	94.2478		52.96
2			50	51	376.9911		212.29
3			51	52	942.4778		81.34
4			52	53	1884.956		24.53
5			53	54	3298.672		16.32
1	16	17	54	55	94.2478		21.48
2			55	56	376.9911		24.6
3			56	57	942.4778		27.59
4			57	58	1884.956		162.62
5			58	59	3298.672		14.23
1	17	18	59	60	94.2478		9.32
2			60	61	376.9911		6.13
3			61	62	942.4778		10.39
4			62	63	1884.956		-----
5			63	64	3298.672		-----
1	18	19	64	65	94.2478		40.48
2			65	66	376.9911		16.91
3			66	67	942.4778		11.77
4			67	68	1884.956		-----
5			68	69	3298.672		-----
1	19	20	69	70	94.2478		16.67
2			70	71	376.9911		6.6
3			71	72	942.4778		-----
4			72	73	1884.956		-----
5			73	74	3298.672		-----
1	20	21	74	75	94.2478		63.64
2			75	76	376.9911		-----
3			76	77	942.4778		-----
4			77	78	1884.956		-----
5			78	79	3298.672		-----

The profile shows an alternation between high and intermediate resistivity zone except towards the far most left with low resistivity zone of <9.94Ωm. The low resistivity zone is produced by the presence of waste water in the soak away present at the area towards the end of the profile line. This section has the highest resistivity zone among all the ERT lines with resistivity range 69.1Ωm to 252Ωm. From the surface it is observed the ground is generally rocky and highly compacted. The area is found to have no foundation problem and it is considered competent.

4. Discussion

The moderately and high resistivity values in the study area component geological materials. This indicates that the higher the resistivity of a given layer, the higher the competence (Akintorin and Adensi, 2009). Also, a group researcher found that subsoils with low resistivity values are most probably porous, less resistive and have high clay content (Olorufemi et al., 2005). In the same vein, some study revealed that the areas that contain near surface low resistivity geological material are highly favorable to pavement failure (Ozegin et al., 2011). This is because these zones are structurally weak, as a result of fracture, favorably disposed to groundwater seepage and accumulation, thus making them low resistivity zones, with great potential for pavement failure. the building with major cracks classified as structural defect were the large lecture Room 4 Block (LLR4) and PG Economics Lab Block (PG EL) with profile of ERT 4 and ERT 6 respectively. Both building have length of 50m and are located closely with one another at the eastern portion of the campus. From the result the areas show low resistivity values of <13.7Ω from the surface to a depth 6m for the ERT 6 and to a depth of 12.4m. the soil in the area is deduced to contain clayey materials. The resistivity variation is deduced to be as a result of the effect of porosity, moisture content and density effect. Other buildings around the eastern part of the campus experience minor cracks which do not necessary counts as structural failure except the LLR4 block and PG Economics Lab block and the study revealed moderate competency for these buildings.

5. Summary

Resistivity of < 20Ωm is considered to represent un-compacted clayey materials. Resistivity of 20Ωm to 40Ωm is considered to represent moderately compacted clayey materials. Resistivity of 70Ωm to 100Ωm is considered to represent highly weathered basement rocks. Resistivity of>100Ωm is considered to represent weathered basement rocks. Un-weathered basement is expected to have resistivity of > 959Ωm because of their poor water storability capacity although no such layer was encounter in this study. The profiles ERT I, ERT 2 and ERT 3 for the geography lab block, Library block and MIS block generally have moderate to high resistivity zones along the profile with only pockets of very low resistive zones not stretching beyond 6m which are accounted for to be voids and waste water. The soil underlying these building is considered to be moderately competent coupled with the fact that there are no apparent cracks on the walls of these buildings. At the ERT 4 (LLR 4) and ERT 6 (PG Economics Lab) line, the soils generally have lower resistivity at the near surface. The ERT 4 (LLR4 Block) line particularly, has the largest zone of low resistivity from the surface to a depth of 9.26m along the traverse. The soil here is considered to be incompetent which has caused several cracks to develop on this building over time. The ERT 5 (Computer Lab) has a moderately competent soil downward to a depth of 9.26m. For the ERT7 line, the region is generally rocky and free of any foundation problem with high resistivity from surface to bottom virtually along the entire traverse.

6. Conclusion

The application of 2D resistivity survey by Dipole-Dipole method and analysis by 2D Electrical Resistivity Tomography (ERT) reveal that resistivity values vary within different rock/soil layers around the buildings investigated. The lithological layers deduced from this study are clayey/lateritic for the first layer and clayey-highly weathered basement and weathered basement. Federal University Lokoja (FULokoja) is situated in a basement terrain. In the campus vicinity, it is observed that the area North of the campus has the highest elevation and the internal structure of the area highly compacted and rocky with shorter depth to the weathered basement soil. With the area being a basement terrain, bedrock will be present at shallow depth which acts to inhibit the percolation of the input of water in the soil by combined action of precipitation, draining, wetting of the grasses making the soil saturated with water. Water remains longer within the soil making it oversaturated which weakens the foundation of the building structures coupled with the presence of high porosity, low density, and clayey material underlining this part of the campus which is susceptible to seasonal shrinking and expansion.

Recommendation

Based on the findings of this study, it is recommended that foundations of subsequent buildings in Federal University Lokoja (FULokoja) should be reinforced by mixing with gravel and Standard Penetration Test (SPT) combined with resistivity survey carried out prior to construction. It is also recommending that proper drainage system be made in the campus to prevent soil saturation.

References

Abdulbariu, I., Izge, H.I., Baba Aminu, M., Ayinla, A.H., 2023. Applications of Vertical Electrical Sounding (VES) and Two-Dimensional (2-D) Imaging Methods for Groundwater Exploration and Basement Configuration at GOFAMINT Church Camp, Ibadan, Southwestern Nigeria. Science Forum (Journal of Pure and Applied Sciences) 23, Pp. 336 – 356.

Aizebeokhai, A.P., Oyeyemi, K.D., 2015. Application of Geoelectrical resistivity imaging and VLF-EM for subsurface characterization in a sedimentary terrain. Southwestern Nigeria. Arab J. Geosci., 8 (6). Pp. 4080-4099.

Akintorinwa, O.J., Ojo, J.S., Olorunfemi, M.O., 2011. Appraisal of the Causes of Pavement Failure Along the Ilesa-Akure Highway, southwestern Nigeria, Using Remotely Sensed and Geotechnical Date, Ife J. Sci., 13 (1), Pp. 185-197.

Akintorinwa, O.J., Ojo, J.S., Olorunfemi, M.O., 2011. Appraisal of the Causes of Pavement Failure Along the Ilesa-Akure Highway, southwestern Nigeria, Using Remotely Sensed and Geotechnical Date, Ife J. Sci., 13 (1), Pp. 185-197.

Aminu, M.B., Nanfa, C.A., Hassan, J.I., Yahuza, I., Christopher, S.D., and Aigbadon, G.O., 2022a. Application of Electrical Resistivity for Evaluation of Groundwater Occurrence Within Adankolo Campus and Environs, Lokoja North Central, Nigeria. European Journal of Environment and Earth Sciences, 3 (1), Pp. 14–22. https://doi.org/10.24018/ejgeo.2022.3.1.235

Aminu, M.B., Nanfa, C.A., Sanni, Z.J., Christopher, S.D., Dahiru, A.T., Ayoola, H.A., and Aigbadon, G.O., 2022b. Hydrocarbon Potential of the South-Western Part of the Cauto Basin, Cuba. European Journal of Environment and Earth Sciences, 3 (1), Pp. 36–47. https://doi.org/10.24018/ejgeo.2022.3.1.242

Andarawus, Y., Nur, A., Musa, N., Adamu, A., Mu'awiya, B.A., 2022. Geoelectrical Investigation for Aquifer Characterization in Boi and Environs, Bauchi State, Northeast, Nigeria. Dutse Journal of Pure and applied Sciences (DUJOPAS), 8 (2a), Pp. 149-170.

Anderson, N., Hoover, R., Sirles, P., 2008. Geophysical methods commonly Employed for the Geochemical Site Characterization. Transportation research Board of the National Academics.

Cardarelli, E., Cercato, M., Di Filipo, G., 2007. Accessing foundation stability and soil-structure interaction through intergrated geophysic tecniques: A case history in Rome (Italy). Near surface Geophysics, 5 (7), Pp. 141-147.

Changde, A.N., Aminu, M.B., Simon, D.C., Ernest, O.A., Kizito, O.M., Godwin, O.A., Okiyi, I.M., 2022. Electric Resistivity for Evaluating Groundwater Potential Along the Drainage Zones in the Part of Jos North, Plateau State, Nigeria. European Journal of Environment and Earth Sciences, (3) 6, Pp. 59-68.

Coseanza, P., Msrmet, E., Rejiba, E., Cui, Y.J., Tabbagh, A., Charlery, Y., 2006. Correlation between geochemical and electrical data: A case study at Garchy in France. Jounal of Applied Geophysics, 60, Pp. 165-178.

Fatoba, J.O., and Salami, B.M., 2004. Geophysical investigation of ground subsidence; A case stydy of a beverage factory site in Edo State, Nigeria. Global J. Geol. Sci., 2 (1), Pp. 153-159.

Ibrahim, A., Baba, A.M., Okechukwu, A.K., 2023. Frequency-Domain Electromagnetic and VLF Data with an Application to Modeling of Basement Structures: A Case Study Within, Ibadan Area, Southwestern Nigeria. (IJRIAS), 8 (6), Pp. 156-175. June DOI: https://doi.org/10.51584/IJRIAS.2023.8616

Ibrahim, A., Izge, H.J., Baba Aminu, M., Osumanu, J., Ayinla, H.A., Appiah, D., Ibrahim, I. O., 2024. Geophysical Characterization of Basement Rock for Groundwater and Mineralization Potential Using Very Low Frequency –

Electromagnetic (VLF-EM) Techniques at Site "G" Around Ibadan Metropolis, Southwestern Basement Complex, Nigeria. Geological Bahavior, 8 (1), Pp. 13-22. DOI: http://doi.org/10.26480/gbr.01.2024.13.22

Mudele, O., Bayer, F.M., Zanandrez, L.F.R., Eiras, A.E., and Gamba, P., 2020. Modeling the Temporal Population Distribution of Ae. aegypti Mosquito Using Big Earth Observation Data, in IEEE Access, 8, Pp. 14182-14194. doi: 10.1109/ACCESS.2020.2966080.

Mudele, O., Frery, A.C., Zanandrez, L.F.R., Eiras A.E., and Gamba, P., 2021. Dengue Vector Population Forecasting Using Multisource Earth Observation Products and Recurrent Neural Networks in IEEE Journal of Selected Topics in Applied Earth Observations and Remote Sensing, 14, Pp. 4390-4404. doi: 10.1109/JSTARS.2021.3073351

Olorunfemi, M.O., Ojo, J.S., Idornige, A.I., Oyetoran, W.E., 2005. Geophysical Investigation of Structural failure of a Factory Site in asaba area, Southern Nigeria. Journal of Minning and Geology, 41 (1), Pp. 111-121.

Onivefu, A.P., 2023. Temperature Programmed Desorption Approach in Understanding the Development of Semiconductors and Catalyst. Communication in Physical Sciences, 10 (1), Pp. 213-229.

Onivefu, A.P., Ikhuoria, E.U., Muniratu, M., Ifijen, I.H., 2024. Exploring the Remarkable Gas Sensing Capability of Molybdenum Diselenide Nanoparticles. In: TMS 2024 153rd Annual Meeting & Exhibition Supplemental Proceedings. TMS 2024. The Minerals, Metals & Materials Series. Springer, Cham. https://doi.org/10.1007/978-3-031-50349-8_3

Roth, J.S., Mackey, J.R., Mackey, C., Nyquist, J.E., 2002. A case study of the reliability of multielectrdde earth resistivity testing for geotechnical investigation in Karst terrains. Eng. Geol. 65, Pp. 225-232.

Salami, B.M., Falebita, D.E., Fatoba, J.O., Ajala, M.O., 2012. Integrated Geophysics and Geotechnical Investigation of bridge Site – A case Study of a Swamp/Creek Environment in Southeast Lagos, Nigeria. Ife J. Sci., 14 (1), Pp. 75-82.

Smith, A.M., Webb, W.L., McBride, T.M., and Siegel, S.B., 2015. The preparation and uses of Sodium, Pp. 22.

Wisen, R., Christiansen, A., Dahlin, T., Auken, E., 2008. Experience from two resistivity inversion tecniques applied in three cases of Geotecnical site investigation. Journal of Geotecnical and Geoenvironmental Engineering, 134 (12), Pp. 1730-1742.